Electronic Supplementary Material (ESI) for Journal of Materials Chemistry C.

Supporting Information

Multi-luminescent centers integrated metal–organic frameworks for high-performance white light-emitting diode

Hailong Wu, Ying Tang, Yuanjing Cui* and Guodong Qian*

State Key Laboratory of Silicon and Advanced Semiconductor Materials, ZJU-Hangzhou Global Scientific and Technological Innovation Center, School of Materials Science and Engineering, Zhejiang University, Hangzhou 310030, China.

E-mail: cuiyj@zju.edu.cn; gdqian@zju.edu.cn

1. Experimental section

1.1 Chemicals and materials

Zinc nitrate hexahydrate ($Zn(NO_3)_2 \cdot 6H_2O$, 99%), lead chloride ($PbCl_2$, 99.999%), lead bromide ($PbBr_2$, 99.999%), lead iodide (PbI_2, 99.999%), oleic acid (OA, AR), oleyl amine (OAm, AR) and organic fluorescent dye SRh101 were purchased from Aladdin Ltd (Shanghai, China). 2-Methylimidazolate (Hmim, 98%) and tetramethyl orthosilicate (TMOS, 98%) were purchased from Energy Chemical. Organic fluorescent dye pm567A was purchased from Exciton (Shanghai, China). Cesium chloride (CsCl, 99.9%), Cesium bromide (CsBr, 99.9%) and Cesium iodide (CsI, 99.9%) were purchased from Xi'an Polymer Light Technology Corp. All the reagents purchased were commercially available and used without further purification.

1.2 Synthesis of ZIF-8, ZIF-8⊃pm567A, ZIF-8⊃SRh101, ZIF-8⊃pm567A/SRh101

The ZIF-8⊃dye nanoparticles were synthesized according to the previous report with minor modifications.[1] A stock solution of organic fluorescent dyes pm567A (0.005 M) and SRh101 (0.005M) in DMF was prepared. 0.2 g $Zn(NO_3)_2 \cdot 6H_2O$ was dissolved in 8 ml methanol and an appropriate amount of organic dyes stock solution was added. Then 10 ml methanol solution containing 0.6g 2-Methylimidazolate was dropwise added into the mixed solution above. ZIF-8⊃dye nanoparticles were generated after three hours of stirring with a rotary speed of 150 r/min, collected by centrifugation, washed with methanol 5 times and dried in air. Pure ZIF-8 was obtained without any addition of organic dye stock solution.

1.3 Synthesis of all-inorganic metal halide perovskite nanocrystals ($CsPbX_3$ NCs)

$CsPbX_3$ NCs were synthesized via room-temperature supersaturated recrystallization (SR) reported by Zeng et al with minor modification.[2] In a typical synthesis of $CsPbClBr_2$ NCs, $PbBr_2$ (0.2 mmol, 73.4 mg) and CsCl (0.2 mmol, 33.7 mg) were added in the solution containing 5 ml DMF, 0.5 ml OA and 0.25 ml OAm, followed by continuous ultrasound until complete dissolution. An appropriate amount of methanol was added to assist in the dissolution of CsCl. Then, 2 ml precursor solution was swiftly added to 10 ml toluene under vigorous stirring. A

pale green solution formed within a few seconds. Other perovskite nanocrystals with different halide compositions were fabricated with a mixture of PbX_2 and CsX (X = Cl, Br, I). The obtained $CsPbX_3$ NCs were washed with toluene via precipitation and redispersed in toluene.

1.4 Synthesis of ZIF-8⊃dye@$CsPbX_3$@SiO_2

ZIF-8⊃dye@$CsPbX_3$@SiO_2 nanocomposites were prepared by mixing the as-obtained ZIF-8 or ZIF-8⊃dye with $CsPbX_3$ NCs and TMOS. In a typical synthesis of ZIF-8⊃pm567A/SRH101@$CsPbClBr_2$@SiO_2, 30 mg ZIF-8⊃pm567A/SRH101 was evenly dispersed to 5 ml toluene with the assistance of ultrasound and then appropriate amount of $CsPbClBr_2$ NCs and 100 μL TMOS was added. After stirring for 12 h, the product was collected by centrifugation, washed with toluene and dried in air. For comparison, a series of ZIF-8 @$CsPbX_3$ was also prepared.

1.5 Determination of the loading amount of $CsPbX_3$ NCs in ZIF-8⊃dye@$CsPbX_3$@SiO_2.

After completing stirring to synthesize ZIF-8⊃dye@$CsPbX_3$@SiO_2, almost all products rapidly settled down within a few minutes and there were few or no apparent $CsPbX_3$ NCs on the supernatant. Based on the fact that the vast majority of $CsPbX_3$ NCs anchored on the surface of ZIF-8⊃dye and subsequently settled with ZIF-8⊃dye particles, we can evaluate the loading amounts of $CsPbX_3$ NCs by simply calculate the mass ratio of $CsPbX_3$ NCs and ZIF-8⊃dye added to the stirring. A certain mass (m) of $CsPbX_3$ NCs was redispersed in toluene with a volume of V_1 to obtain a stock solution. Based on the above analysis, the loading amount of $CsPbX_3$ NCs of ZIF-8⊃dye@$CsPbX_3$@SiO_2 can be expressed to be $\omega = (m\times V_2/V_1)/(M+m\times V_2/V_1)$, where V_2 and M represent the volume of the stock solution of $CsPbX_3$ NCs and the mass of ZIF-8⊃dye, respectively. For $CsPbClBr_2$ NCs, the m, M and V_1 were determined as 5.1 mg, 30 mg, and 20 mL, respectively. Therefore, the appropriate volume (V_2) of this stock solution was added to obtain ZIF-8⊃dye@$CsPbClBr_2$@SiO_2 with a desirable loading amount of $CsPbClBr_2$ NCs. For example, when 100 μL stock solution of $CsPbClBr_2$ NCs was added, the loading amount can be calculated to be 0.085 wt%.

1.6 Fabrication of LEDs

The prototype white LEDs were fabricated by coating intimate mixtures of ZIF-8⊃dye@$CsPbX_3$@SiO_2 and transparent epoxy resin on a commercial blue-LED chip (λ_{max} = 460 nm). CRI, CIE and CCT were calculated by "Chameleon-Spectrum" software.

1.7 Measurements

Powder X-ray diffraction (PXRD) patterns were collected on an X'Pert PRO diffractometer with Cu Kα radiation (λ = 1.542 Å) at room temperature, in the range of 2θ = 5-50º. The morphology was investigated using field-emission scanning electron microscopy (FE-SEM, Hitachi S4800). Transmission electron microscope imaging and STEM-EDS were performed on the HRTEM (Tecnai G2 F20 S-TWIN, FEI) operating at an acceleration voltage of 100 kV. UV-vis absorption spectroscopy was measured with a UV-2600 UV-vis spectrophotometer (Shimadzu, Japan). The Steady-state fluorescence spectrum was obtained on a Hitachi F-4600 fluorescence spectrometer at room temperature. The quantum yields were recorded on an Edinburgh Instrument F920 spectrometer.

2. Supporting Tables and Figures

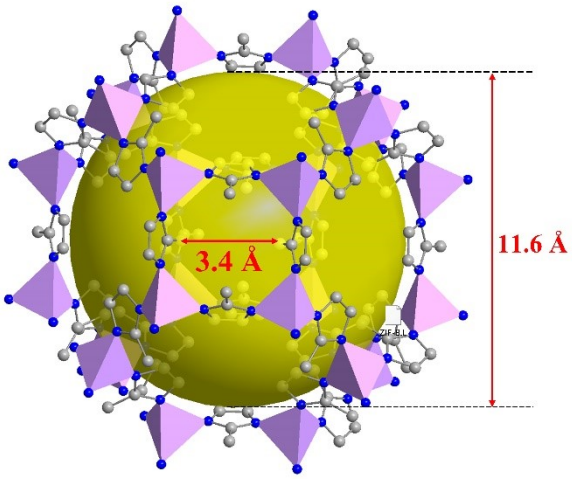

Figure S1. Single-crystal structure of ZIF-8, where the aperture and cage sizes are indicated.

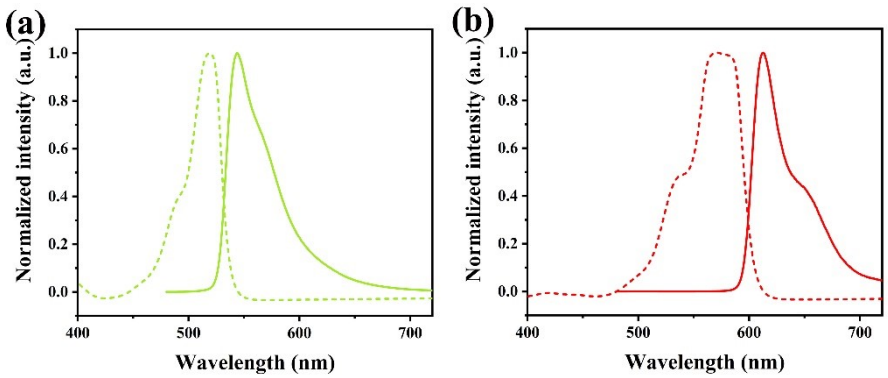

Figure S2. The UV–vis absorption spectra (dashed line) and emission spectra (solid line) of (a) ZIF-8⊃pm567A and (b) ZIF-8⊃SRh101, respectively.

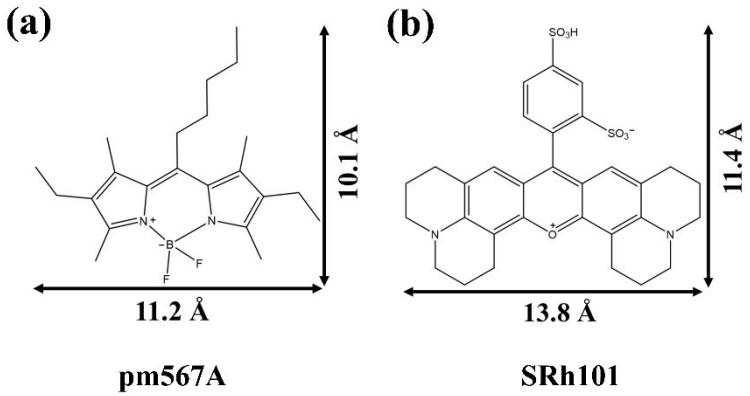

Figure S3. Chemical structures of (a) pm567A and (b) SRh101 with the corresponding molecular dimensions

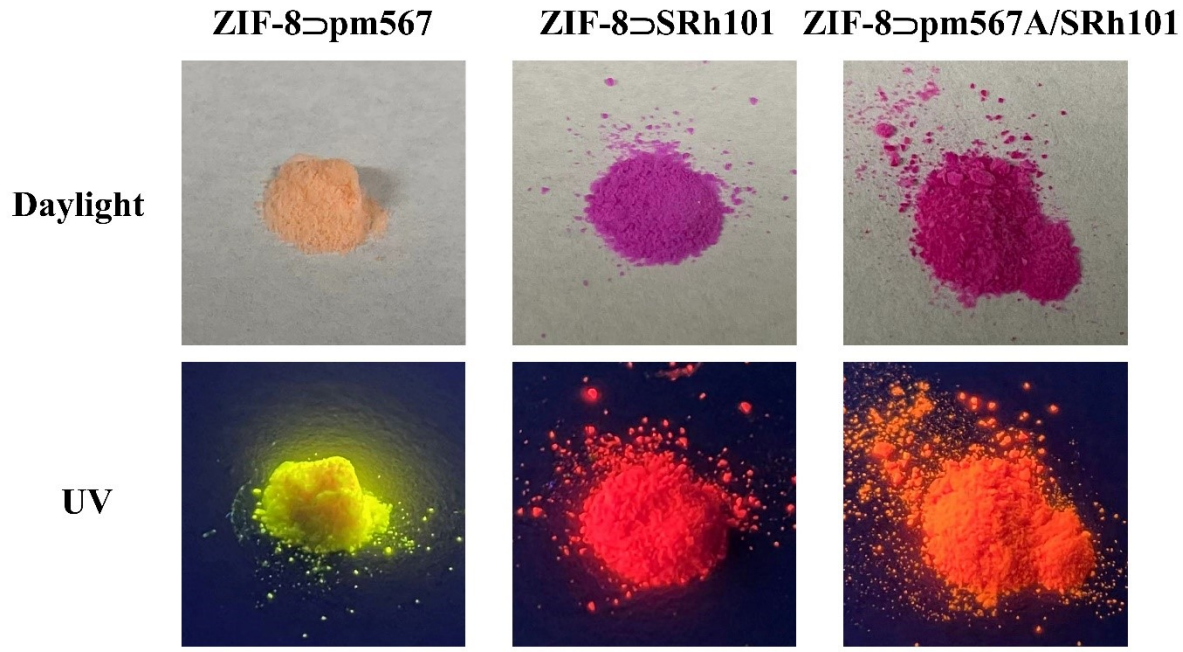

Figure S4. Photographs of ZIF-8⊃pm567A, ZIF-8⊃SRh101 and ZIF-8⊃pm567A/SRh101 under daylight and UV.

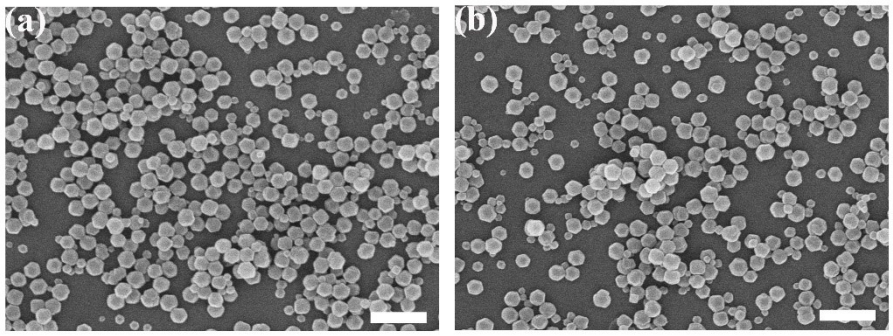

Figure S5. The SEM images of (a) ZIF-8 and (b) ZIF-8⊃pm567A/SRh101. Scale bar, 500 nm.

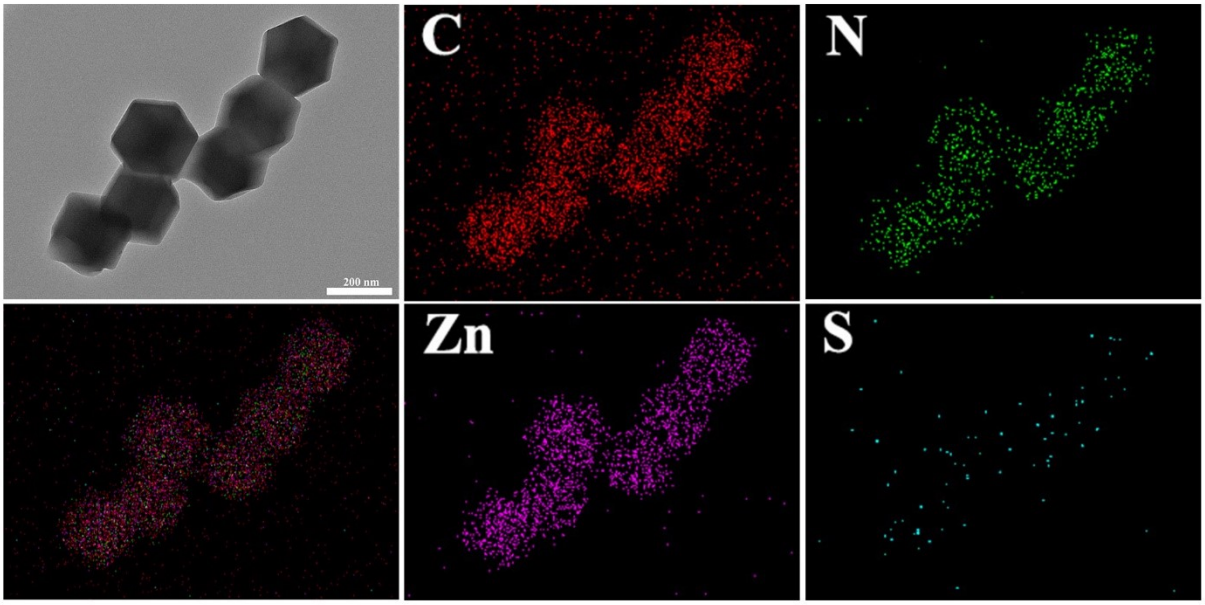

Figure S6. The TEM image of ZIF-8⊃pm567A/SRh101 and the corresponding elemental mapping diagrams of C, N, Zn and S.

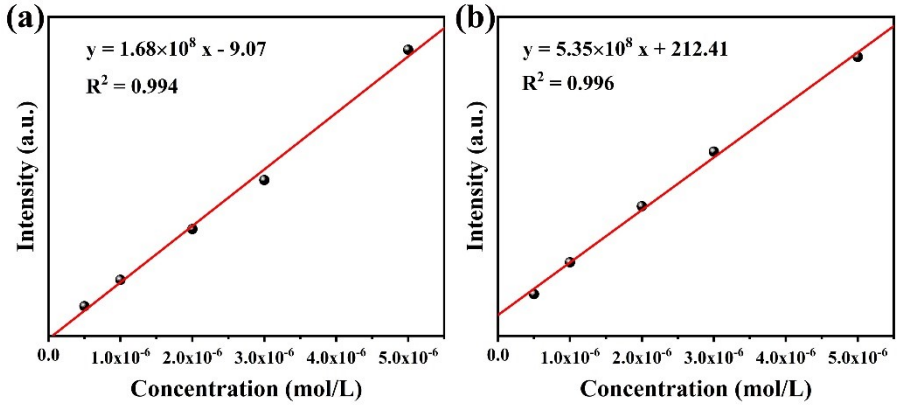

Figure S7. The intensity-concentration relationship of (a) pm567A and (b) SRh101 in dilute solution.

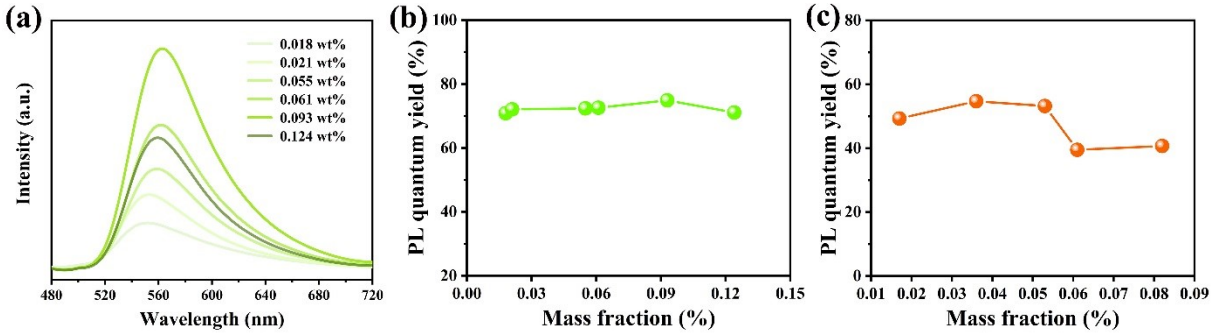

Figure S8. (a) The emission spectra and (b) corresponding PLQYs of ZIF-8⊃pm567A with different loading amounts of pm567A; (c) The PLQYs of ZIF-8⊃pm567A/SRh101 with fixed loading amounts of pm567A and different loading amounts of SRh101.

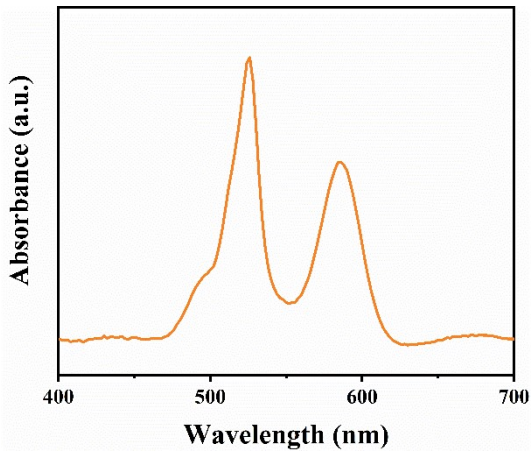

Figure S9. The UV-vis spectrum of ZIF-8⊃pm567A/SRh101 with 0.093 wt% pm567A and 0.053 wt% SRh101.

Figure S10. A photograph of an LED fabricated by ZIF-8⊃pm567A/SRh101 with a 460 nm blue LED chip.

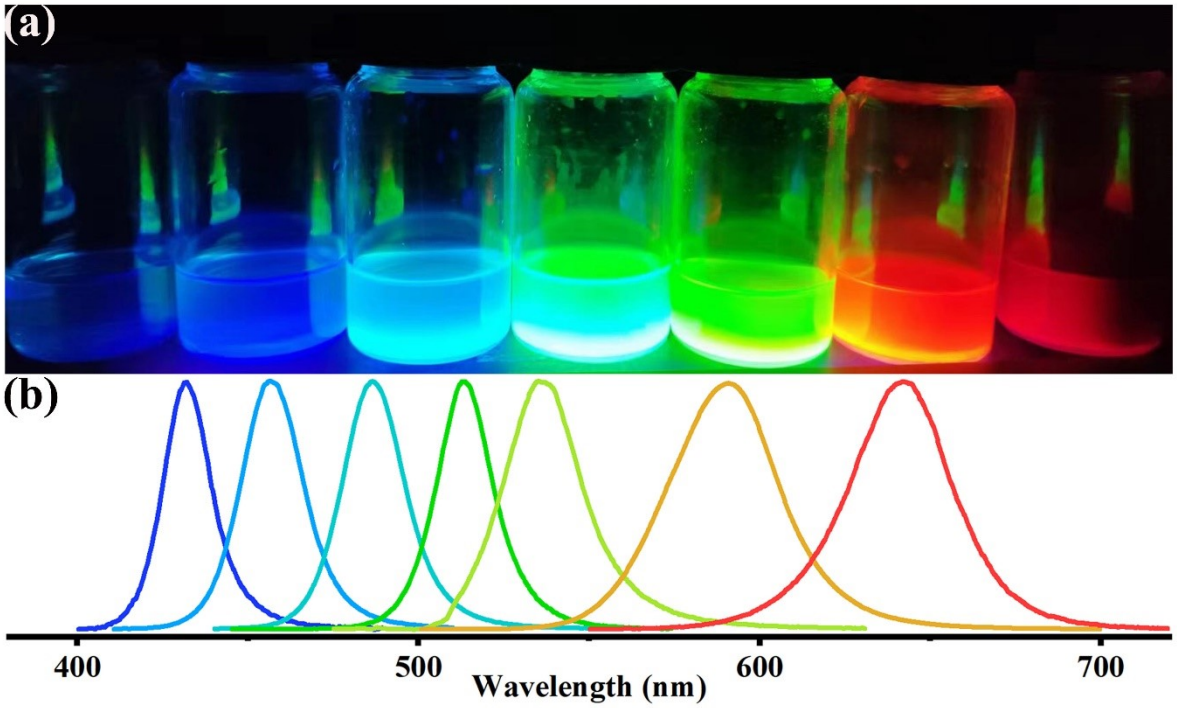

Figure S11. (a) The photograph and (b) corresponding emission spectra of $CsPbX_3$ NCs.

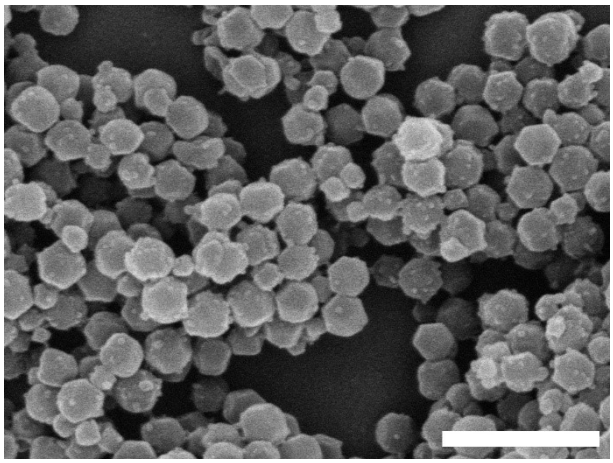

Figure S12. The SEM image of ZIF-8⊃pm567A/SRh101@$CsPbClBr_2$.

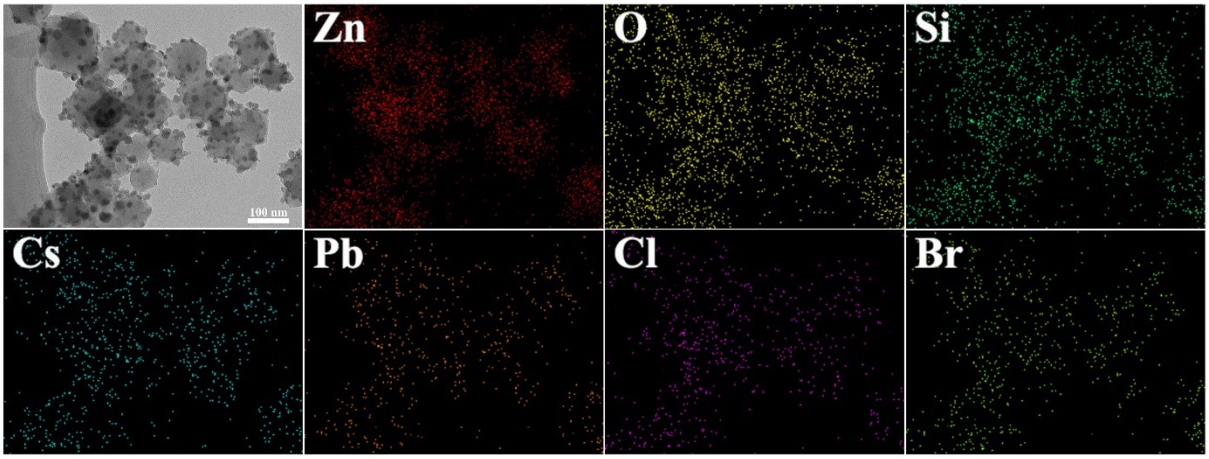

Figure S13. The TEM image of ZIF-8⊃pm567A/SRh101@$CsPbClBr_2$-SiO_2 and the corresponding elemental mapping diagrams of Zn, O, Si, Cs, Pb, Cl and Br.

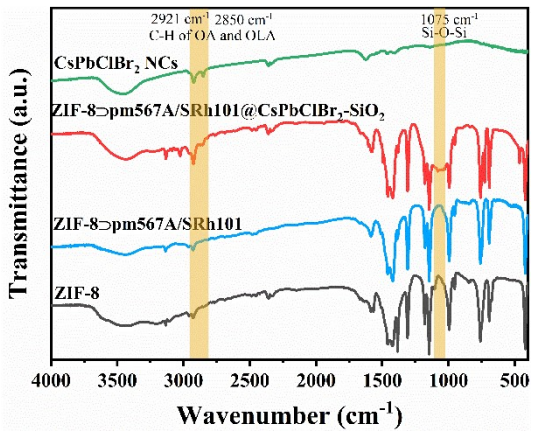

Figure S14. FTIR spectra of ZIF-8, ZIF-8⊃pm567/SRh101, $CsPbClBr_2$ NCs and ZIF-8⊃pm567A/SRh101@$CsPbClBr_2$-SiO_2.

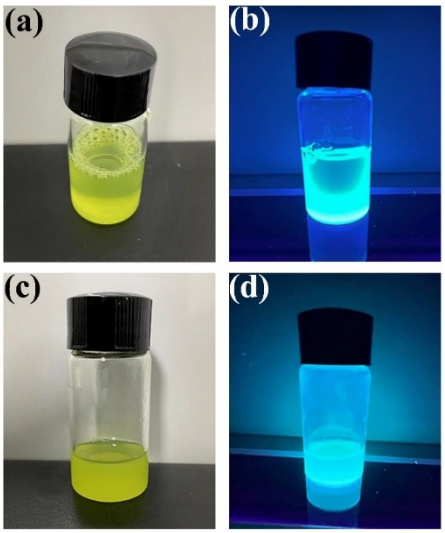

Figure S15. Photographs of (a, b) $CsPbClBr_2$ NCs and (c, d) ZIF-8 @$CsPbClBr_2$-SiO_2 under daylight and UV.

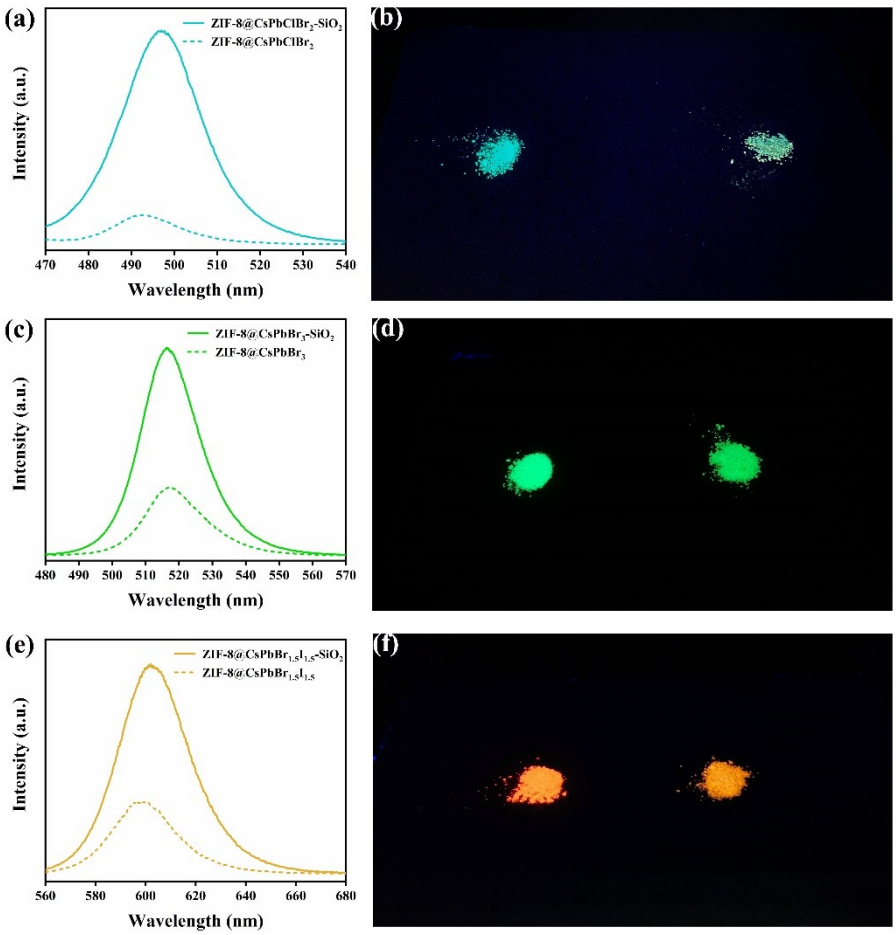

Figure S16. The emission spectra and photographs of (a, b) ZIF-8@$CsPbClBr_2$-SiO_2, (c, d) ZIF-8@$CsPbBr_3$-SiO_2 and (e, f) ZIF-8@$CsPbClBr_{1.5}I_{1.5}$-SiO_2.

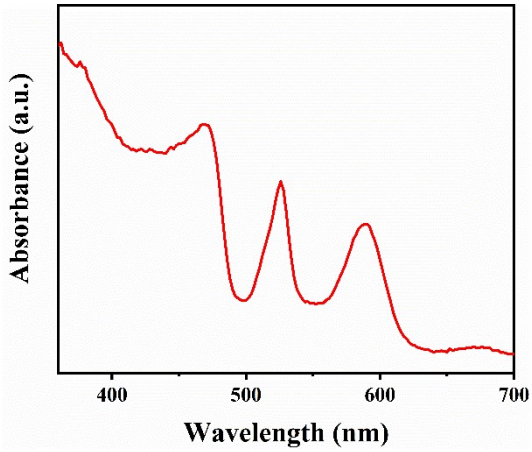

Figure S17. The UV-vis spectrum of ZIF-8⊃pm567A/SRh101@$CsPbClBr_2$-SiO_2.

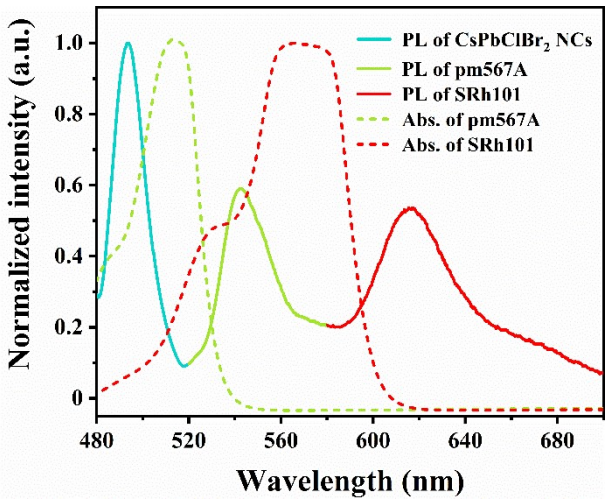

Figure S18. The UV–vis absorption spectra (dashed line) and emission spectra (solid line) of pm567A, SRh101 and $CsPbClBr_2$ NCs, respectively.

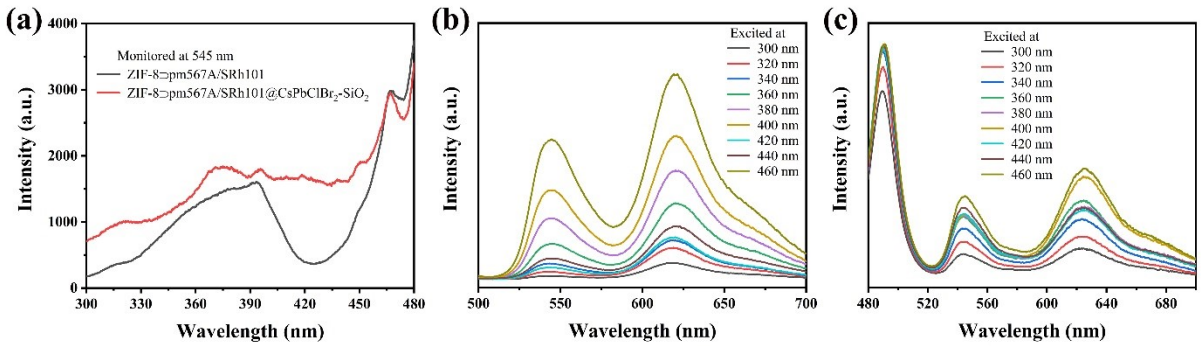

Figure S19. (a) The excitation spectra of ZIF-8⊃pm567A/SRh101@$CsPbClBr_2$-SiO_2 and ZIF-8⊃pm567A/SRh101 with the monitor wavelength of 545 nm. (b) The excitation-wavelength-dependent emission spectrum of ZIF-8⊃pm567A/SRh101. (c) The excitation-wavelength-dependent emission spectrum of ZIF-8⊃pm567A/SRh101@$CsPbClBr_2$-SiO_2.

According to the recent relevant review, a reliable proof of the energy transfer can be obtained by measuring the excitation spectrum, selecting the emission (observation) wavelength in a region where the emission of the acceptor can be detected, but where there is no emission signal from the donor.[3] We have measured the excitation spectra of ZIF-8⊃pm567A/SRh101 and ZIF-8⊃pm567A/SRh101@$CsPbClBr_2$-SiO_2 by selecting 545 nm as

the monitor wavelength. When using the emission of pm567A (545 nm) as the monitor wavelength, ZIF-8⊃pm567A/SRh101 cannot be effectively excited within the wavelength range of 400-450 nm while ZIF-8⊃pm567A/SRh101@$CsPbClBr_2$-SiO_2 can be effectively excited within this wavelength range. Therefore, we attributed this to the strong absorption of $CsPbClBr_2$ NCs in this wavelength range and the energy transfer from $CsPbClBr_2$ NCs to pm567A.

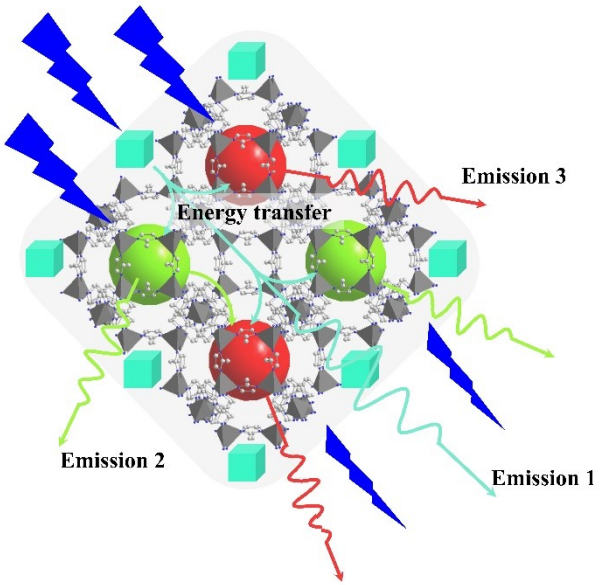

Figure S20. Illustration of the energy transfer in ZIF-8⊃pm567A/SRh101@$CsPbClBr_2$-SiO_2.

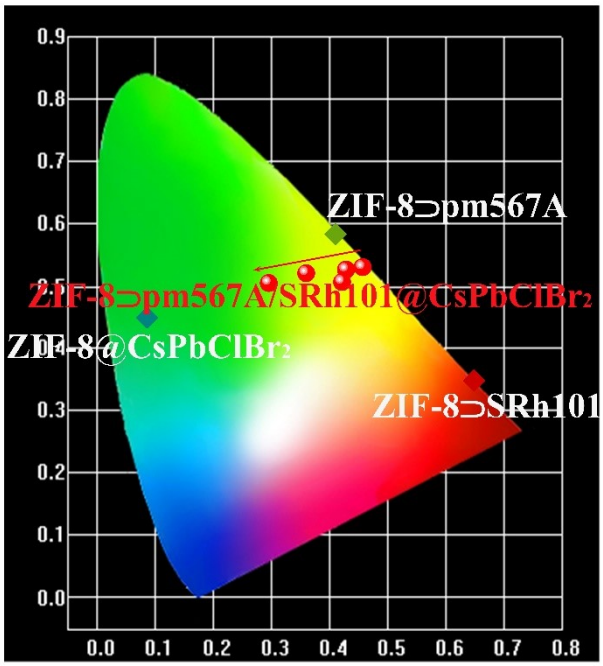

Figure S21. The CIE chromaticity coordinates of ZIF-8⊃pm567A/SRh101@$CsPbClBr_2$-SiO_2 with fixed loading amounts of pm567A and SRh101and different loading amounts of $CsPbClBr_2$ NCs.

Figure S22. A photograph of an LED fabricated by ZIF-8⊃pm567A/SRh101@$CsPbClBr_2$-SiO_2 with a 460 nm blue LED chip.

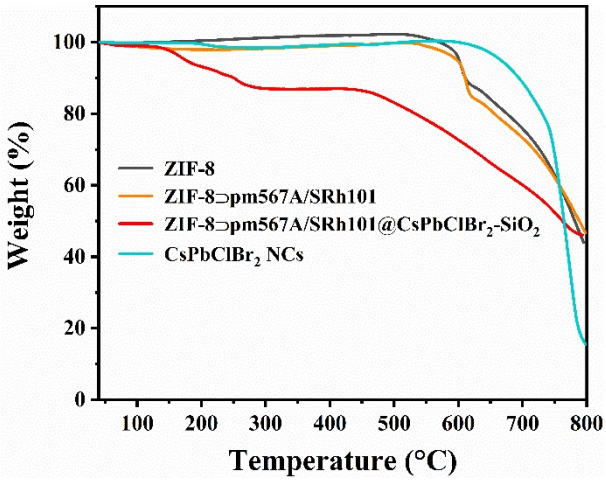

Figure S23. The thermogravimetric curves of ZIF-8, ZIF-8⊃pm567A/SRh101, ZIF-8⊃pm567A/SRh101@$CsPbClBr_2$-SiO_2 and $CsPbClBr_2$ NCs.

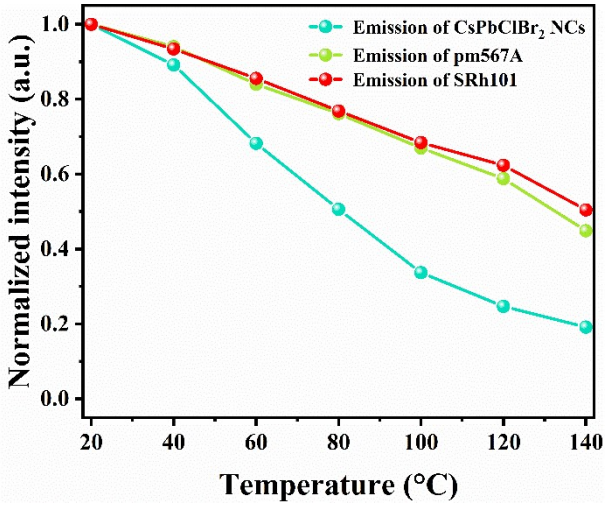

Figure S24. The thermostability of ZIF-8⊃pm567A/SRh101@$CsPbClBr_2$-SiO_2.

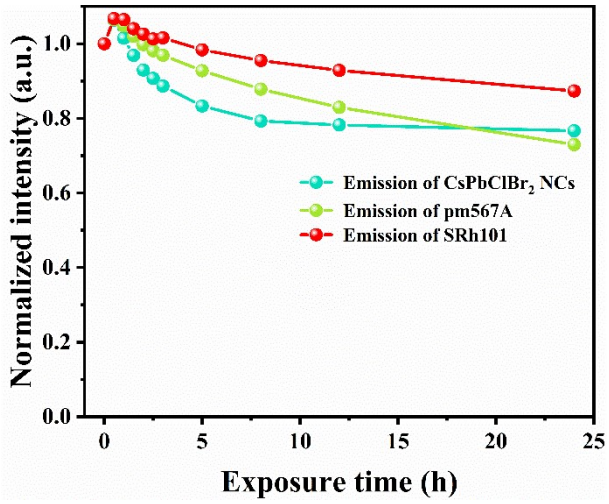

Figure S25. The photostability of ZIF-8⊃pm567A/SRh101@$CsPbClBr_2$-SiO_2.

Table S1. PLQYs of ZIF-8⊃pm567A with different loading amounts of pm567A.

Sample	PLQY (%)
ZIF-8⊃pm567A (0.018 wt% pm567A)	70.9
ZIF-8⊃pm567A (0.021 wt% pm567A)	72.1
ZIF-8⊃pm567A (0.055 wt% pm567A)	72.4
ZIF-8⊃pm567A (0.061 wt% pm567A)	72.6
ZIF-8⊃pm567A (0.093 wt% pm567A)	74.9
ZIF-8⊃pm567A (0.124 wt% pm567A)	71.1

Table S2. The PLQYs of ZIF-8⊃pm567A/SRh101 with fixed loading amounts of pm567A and different loading amounts of SRh101.

Sample	PLQY (%)
ZIF-8⊃pm567A/SRh101 (0.017 wt% SRh101)	49.3
ZIF-8⊃pm567A/SRh101 (0.036 wt% SRh101)	54.7
ZIF-8⊃pm567A/SRh101 (0.053 wt% SRh101)	53.2
ZIF-8⊃pm567A/SRh101 (0.061 wt% SRh101)	39.5
ZIF-8⊃pm567A/SRh101 (0.082 wt% SRh101)	40.7

Table S3. The PLQYs of ZIF-8⊃pm567A/SRh101@$CsPbClBr_2$-SiO_2 with different loading amounts of $CsPbClBr_2$ NCs.

Sample	PLQY (%)
ZIF-8⊃pm567A/SRh101@$CsPbClBr_2$-SiO_2 (0.013 wt% $CsPbClBr_2$)	44.2
ZIF-8⊃pm567A/SRh101@$CsPbClBr_2$-SiO_2 (0.037 wt% $CsPbClBr_2$)	45.7
ZIF-8⊃pm567A/SRh101@$CsPbClBr_2$-SiO_2 (0.085 wt% $CsPbClBr_2$)	45.8
ZIF-8⊃pm567A/SRh101@$CsPbClBr_2$-SiO_2 (0.140 wt% $CsPbClBr_2$)	44.8
ZIF-8⊃pm567A/SRh101@$CsPbClBr_2$-SiO_2 (0.179 wt% $CsPbClBr_2$)	43.6
ZIF-8⊃pm567A/SRh101@$CsPbClBr_2$-SiO_2 (0.217 wt% $CsPbClBr_2$)	42.1

3. References

1. H. Zheng, Y. Zhang, L. Liu, W. Wan, P. Guo, A. M. Nyström and X. Zou, *J. Am. Chem. Soc.*, 2016, **138**, 962-968.
2. X. Li, Y. Wu, S. Zhang, B. Cai, Y. Gu, J. Song and H. Zeng, *Adv. Funct. Mater.*, 2016, **26**, 2435-2445.
3. M. Gutiérrez, Y. Zhang and J.-C. Tan, Chem. Rev., 2022, **122**, 10438-10483.